

# Supplementary Materials for Defining an Essential Transcription Factor Program for Naïve Pluripotency

Authors: S-J Dunn, G Martello, B Yordanov, S Emmott, AG Smith

correspondence to: [graziano.martello@unipd.it](mailto:graziano.martello@unipd.it), [austin.smith@cscr.cam.ac.uk](mailto:austin.smith@cscr.cam.ac.uk)

Figures S1-S6

1: Materials and Methods

- A. [Embryonic Stem Cell Culture](#)
- B. [Gene Expression Analysis by Quantitative RT-PCR with Reverse Transcription](#)
- C. [RNAi Experiments](#)
- D. [Flow Cytometry](#)
- E. [ChIP-seq and Microarray Data Analysis](#)
- F. [Computational Approach](#)
- G. [Abstract Boolean Networks](#)
- H. [Reasoning about Abstract Boolean Networks](#)
- I. [Reasoning Engine for Interaction Networks \(RE:IN\)](#)
- J. [An ABN model of the Pluripotency Network](#)
- K. [Encoding Experimental Behaviour](#)
- L. [Model Predictions](#)
- M. [Refining the Meta-Model](#)
- N. [Minimal Model](#)

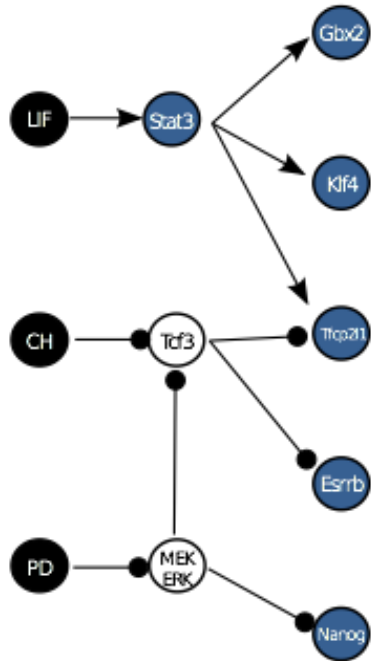
2: Supplementary Text

- A. [Initial Validation of Possible Network Interactions](#)
- B. [Non-intuitive predictions](#)
- C. [Extended Discussion](#)

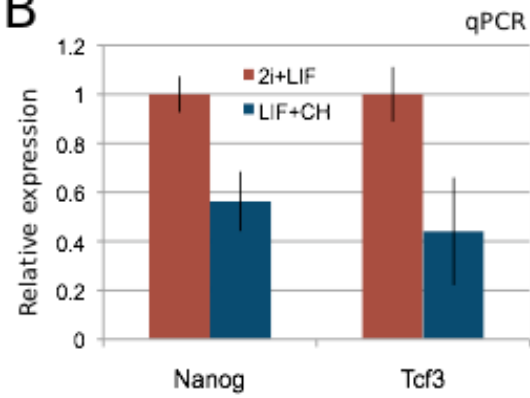
Tables S1-S3

Figure S1

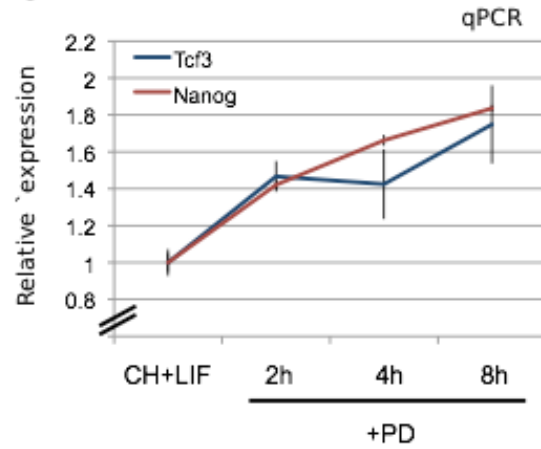
A



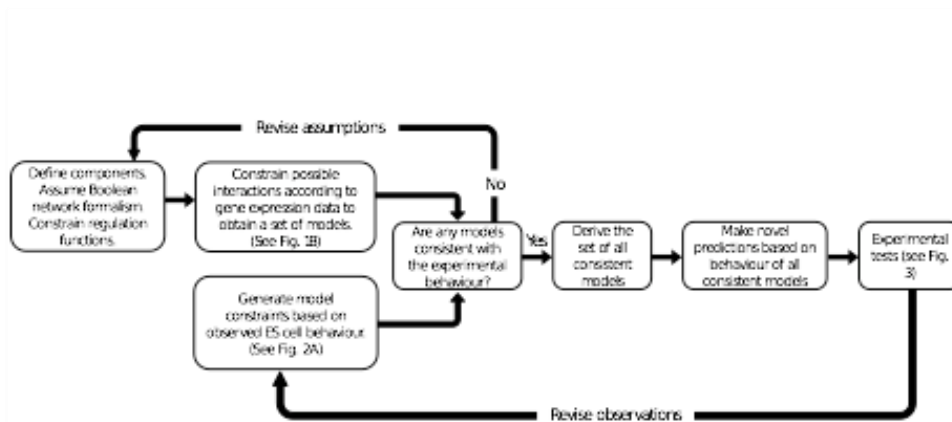
B



C

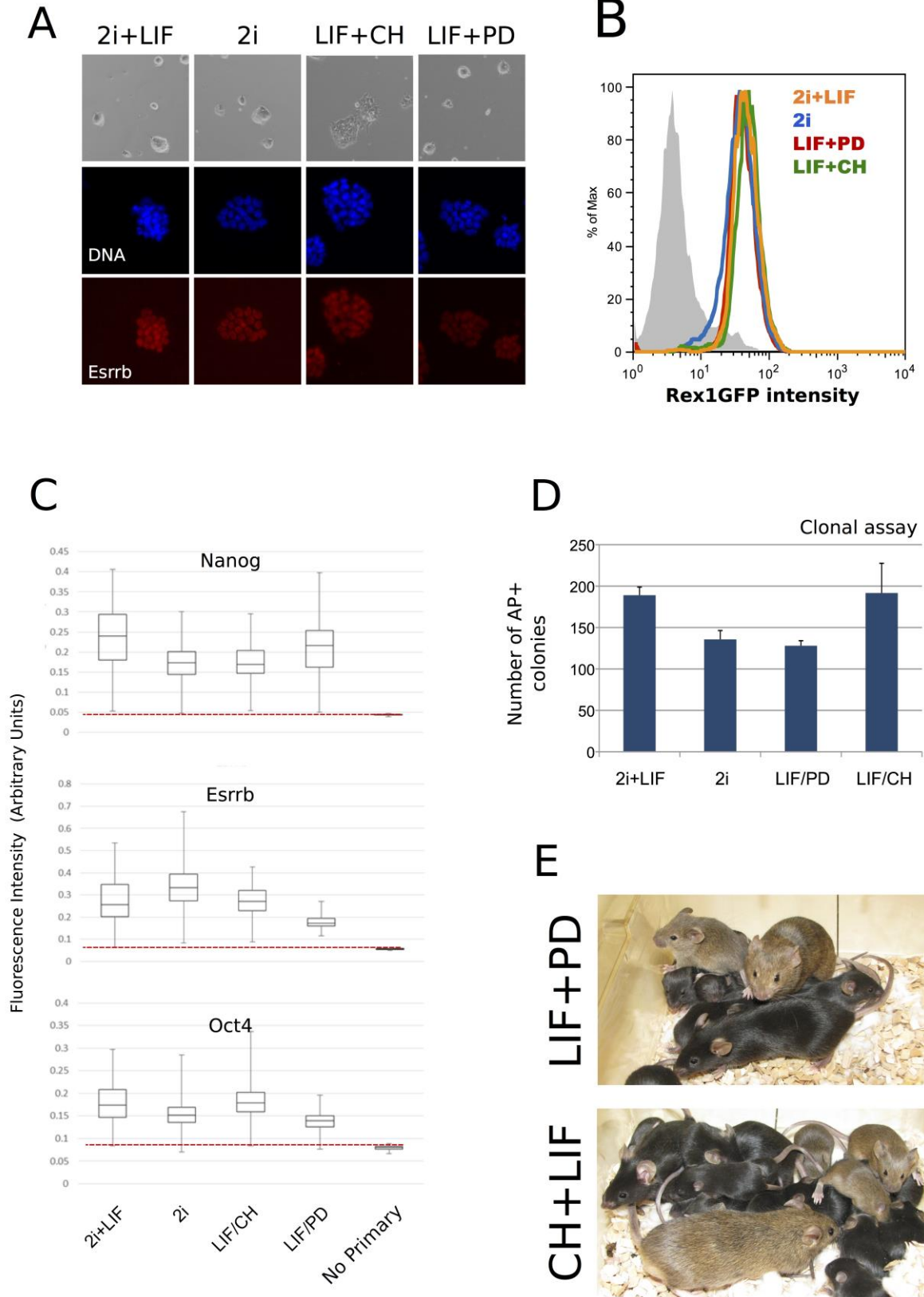


D



**Supplementary Fig. S1:** (A) Schematic showing the direct targets of Stat3, Tcf3 and Mek/Erk. LIF activates expression of the transcription factor Stat3, which, in turn, activates Klf4 (1), Gbx2 (2) and Tfcp2l1 (3). GSK3 inhibition by CH has been shown to stabilise the ES cell state via abrogation of T-cell factor 3 (Tcf3) (4). Esrrb and Tfcp2l1 have been identified as a direct functional targets of Tcf3 (5). ES cell differentiation involves stimulation of the mitogen-activated protein kinase (ERK1/2) pathway by fibroblast growth factor-4 (FGF4), and blockade of this pathway is achieved using PD (6). The downstream targets of MEK/ERK are Nanog and Tcf3 (7, 8) (see panels B and C). **(B)** Gene-expression analysis of ES cells cultured in presence of LIF+CH (blue bars) or 2i+LIF (red bars) for 10 days. Note that PD significantly increases the expression of both Nanog and Tcf3. ActinB served as a loading control, and bars indicate the mean and SD of two independent experiments. **(C)** Gene-expression analysis of ES cells cultured in presence of LIF+CH for 10 days, exposed for the indicated time to PD. Note that PD significantly increases the expression of both Nanog and Tcf3 after 2h. ActinB served as a loading control and bars indicate the mean and SD of two independent experiments. **(D)** In order to determine the essential interactions required in the pluripotency program we followed the illustrated workflow. First, we inferred optional interactions from gene expression data (Fig. 1B) and thereby constructed a meta-model of the network. Known experimental behaviour of ES cells was used to constrain this set (Fig. 2A), which was subsequently used to make predictions of ES cell behaviour in response to genetic perturbations. The predictions were experimentally tested (Fig. 3). This approach can be iterated to incorporate new experimental results and refine the model.

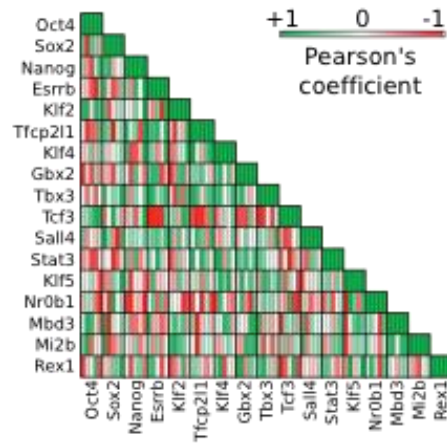
Figure S2



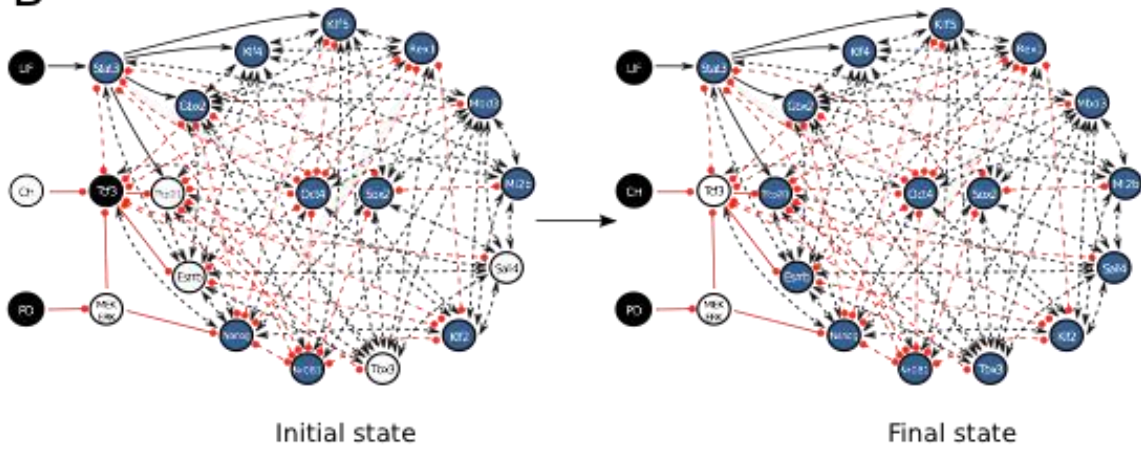
**Supplementary Fig. S2:** (A) Culture conditions used to maintain pluripotency *in vitro*: any two of LIF, CH and PD (together '2i') are sufficient to prevent differentiation. Top panels show the undifferentiated morphology. Bottom panels show immunostaining for the naïve pluripotency marker Esrrb. (B) Under the four different culture conditions, ES cells homogeneously express the Rex1GFP pluripotency marker. 72h after signal withdrawal the majority of cells downregulate the reporter (profile in grey). (C) Box-whisker plots showing the fluorescence immunostaining intensity for Nanog, Oct4 and Esrrb in ES cells cultured under each of the four conditions. As a negative control cells were stained without primary antibody incubation. The red dashed lines indicate the fluorescence intensity measured in the negative control. Under the four different culture conditions >97% of cells expressed the indicated pluripotency markers. This is in stark contrast to previous reports (Niwa et al, 2009 *Nature*; Martello et al, 2012 *Cell Stem Cell*) where the naïve markers Nanog and Esrrb were expressed by only ~50% of cells cultured in LIF+Serum. Boxes show the first, second and third quartile, whiskers show the maximum and minimum value. See Table S3 for the list of antibodies and conditions used. (D) Colony formation in the indicated culture conditions. Cells were cultured for 10 days and plated at clonal density (500 cells for each well). The number of undifferentiated AP+ colonies obtained 5 days after plating is indicated. Bars show mean and SD (n=3). (E) Chimaera formation and germline transmission. ES cells were cultured in either LIF+CH or LIF+PD for 2 weeks before blastocyst injection. Representative images of high contribution chimeras and offspring are shown. The presence of brown pups indicates germ-line transmission. Black siblings are included for comparison. Chimera formation from 2i or 2i+LIF cultures was previously reported (11, 12, 17).

Figure S3

A

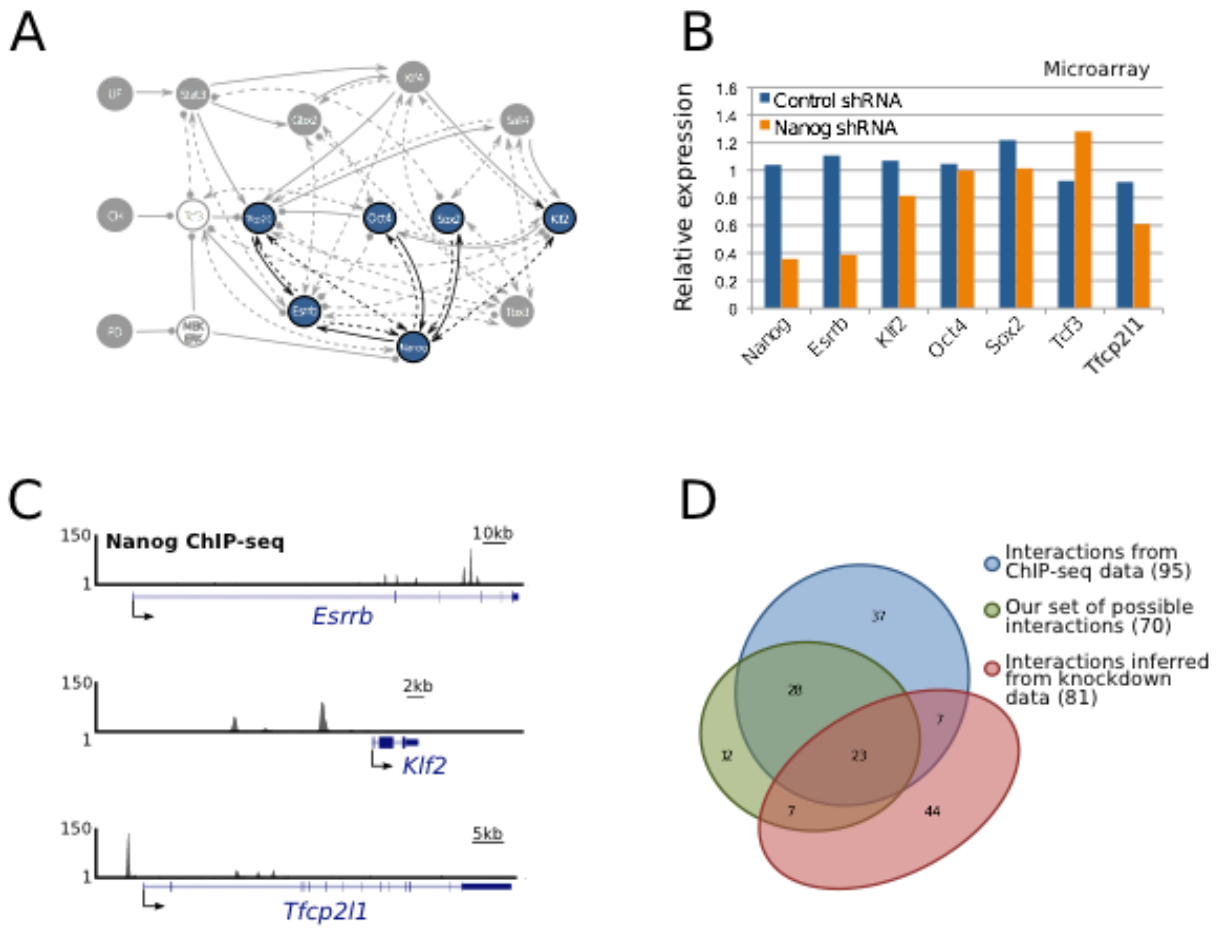


B



**Supplementary Fig. S3:** (A) Pearson correlation coefficients are generated for each gene pair for each of the five experiments in Fig. 1B. The variation in Pearson coefficients for each gene pair is shown. (B) The optional interactions inferred from the experimental data in Fig. 1B for an initial Pearson coefficient threshold of 0.7, and the expected gene expression for conditions of LIF+PD (left) and 2i+LIF (right). Gene expression is discretised to high (blue) or low (white). Positive regulation is shown as a black arrow, while negative regulation is shown as a red circle-headed line. Dashed lines indicate optional interactions, solid lines indicate definite interactions: these are direct downstream targets of Stat3, Tcf3 and MEK/ERK that have been previously experimentally validated (see Fig. S1) (1–3, 5, 7, 8).

Figure S4





**Supplementary Fig. S4:** (A) Based on our gene expression data, there are 6 possible positive interactions that involve Nanog, which are highlighted. (B) Microarray data reveals the effect of a single knockdown of Nanog on these 6 genes. Only 3 genes, Esrrb, Klf2 and Tfcp2l1, show a mild downregulation upon Nanog knockdown. (C) Nanog ChIP-Seq data reveals that Nanog directly binds Esrrb, Klf2 and Tfcp2l1 gene loci. (D) Venn diagram of the overlap in the possible interactions independently inferred from ChIP-Seq data, knockdown experiments and our gene expression data. Only 12 of our interactions are not validated and represent previously unsuspected relationships. In addition these alternative data sets suggest interactions that we do not consider. However, we show that these additional interactions are not required to satisfy the constraints shown in Fig. 2B.

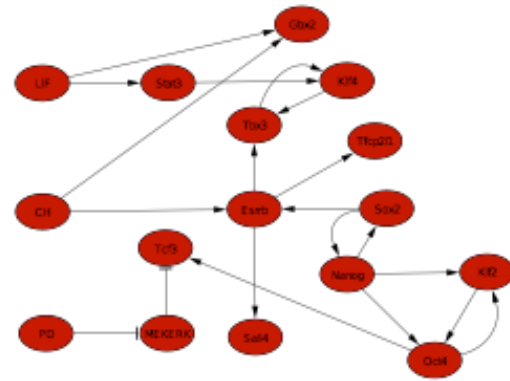
# Figure S5

A

■ Positive regulation  
■ Negative regulation  
■ Binding

Source	Target	Our data	Knockdown data	ChIP-Seq	Bayesian approach
Esr1b	Klf2				
Klf2	Esr1b				
Esr1b	Klf4				
Klf4	Esr1b				
Esr1b	Nanog				
Nanog	Esr1b				
Esr1b	Oct4				
Oct4	Esr1b				
Esr1b	Tbx3				
Tbx3	Esr1b				
Esr1b	Tfcp2l1				
Tfcp2l1	Esr1b				
Esr1b	Stat3				
Stat3	Esr1b				
Esr1b	Gbx2				
Gbx2	Esr1b				
Klf2	Klf4				
Klf4	Klf2				
Klf2	Nanog				
Nanog	Klf2				
Klf2	Oct4				
Oct4	Klf2				
Klf2	Tbx3				
Tbx3	Klf2				
Klf2	Tfcp2l1				
Tfcp2l1	Klf2				
Klf2	Gbx2				
Gbx2	Klf2				
Klf2	Sox4				
Sox4	Klf2				
Klf2	Tcf3				
Tcf3	Klf2				
Klf4	Tbx3				
Tbx3	Klf4				
Klf4	Tfcp2l1				
Tfcp2l1	Klf4				
Klf4	Gbx2				
Gbx2	Klf4				
Nanog	Oct4				
Oct4	Nanog				
Nanog	Tfcp2l1				
Tfcp2l1	Nanog				
Nanog	Sox2				
Sox2	Nanog				
Oct4	Tfcp2l1				
Tfcp2l1	Oct4				
Oct4	Gbx2				
Gbx2	Oct4				
Oct4	Tcf3				
Tcf3	Oct4				
Tbx3	Tfcp2l1				
Tfcp2l1	Tbx3				
Tbx3	Gbx2				
Gbx2	Tbx3				
Tbx3	Sox4				
Sox4	Tbx3				
Tbx3	Tcf3				
Tcf3	Tbx3				
Tbx3	Sox2				
Sox2	Tbx3				
Tfcp2l1	Sox4				
Sox4	Tfcp2l1				
Stat3	Tcf3				
Tcf3	Stat3				
Stat3	Sox2				
Sox2	Stat3				
Sox4	Sox2				
Sox2	Sox4				
Tcf3	Nanog				
Nanog	Tcf3				
Oct4	Sox2				
Sox2	Oct4				
Percentage overlap			44.4%	74%	15.3%

B



**Supplementary Fig. S5:** (A) A summary of the interactions inferred using a Pearson correlation coefficient threshold of 0.792, with the additional optional positive Oct4/Sox2 interaction that is required to correct the incorrect prediction for conditions of 2i+LIF. This summary indicates whether these interactions are supported by microarray data after TF knockdown, ChIP-Seq binding data, or a model obtained using Bayesian inference methods (9). Blank indicates that the interaction is not suggested by these data / approach. (B) Model obtained applying a Bayesian network inference method, previously used to study somatic cell reprogramming (10), to our gene expression data. Arrows indicate positive regulations, whereas negative regulations are shown as blunted lines. Note that in this model there are no external inputs to Oct4, Sox2 or Nanog.

# Figure S6

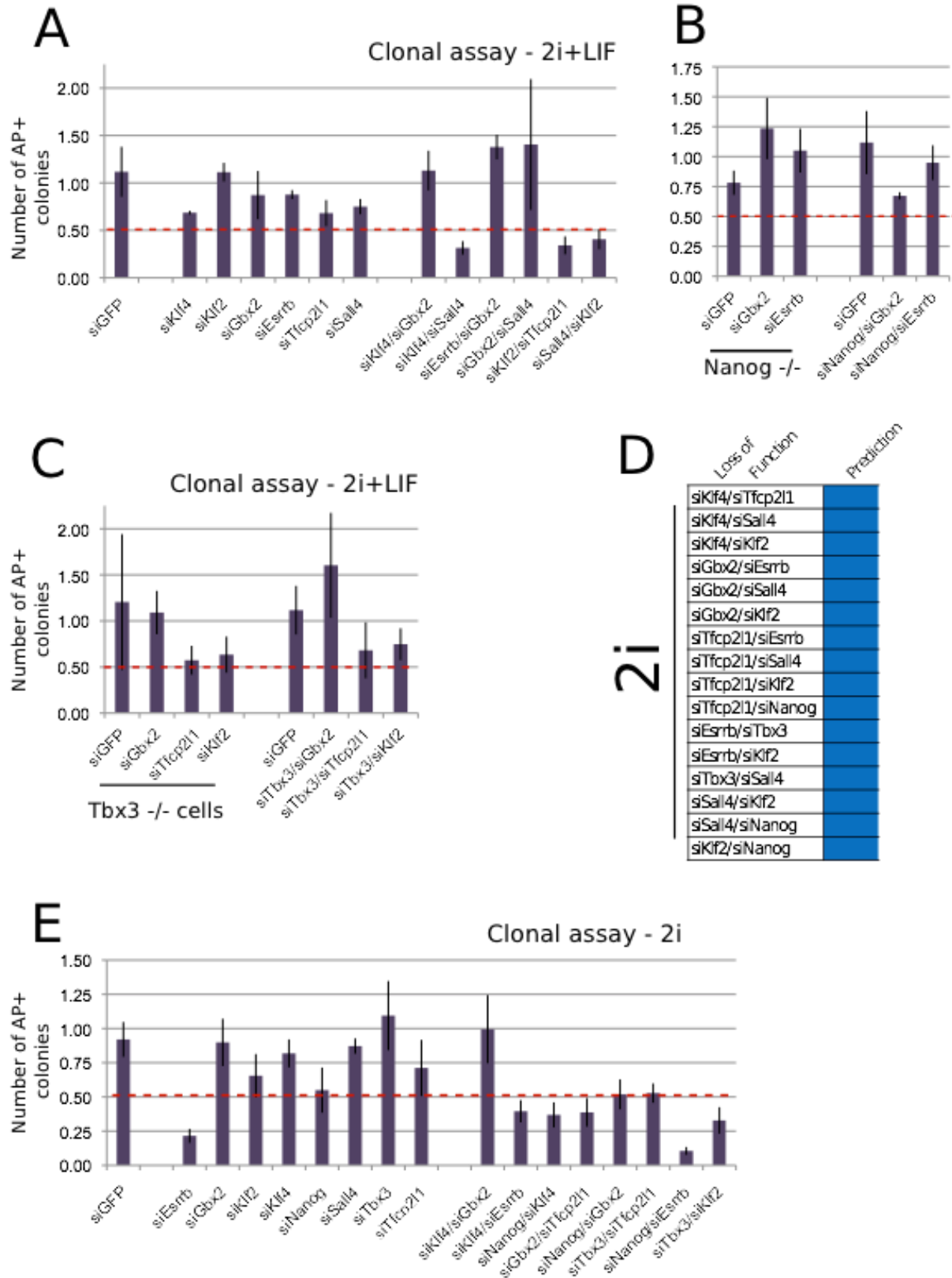
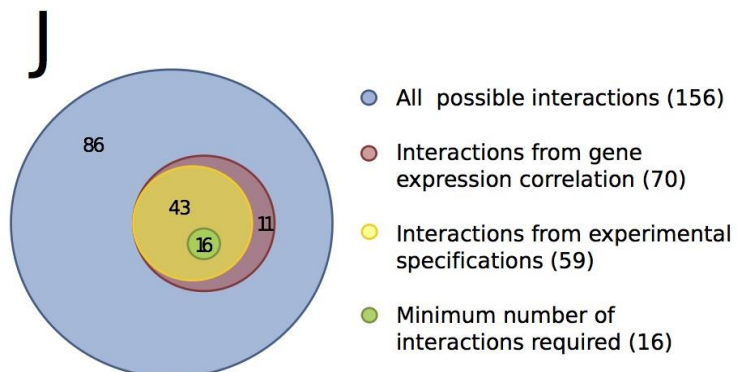
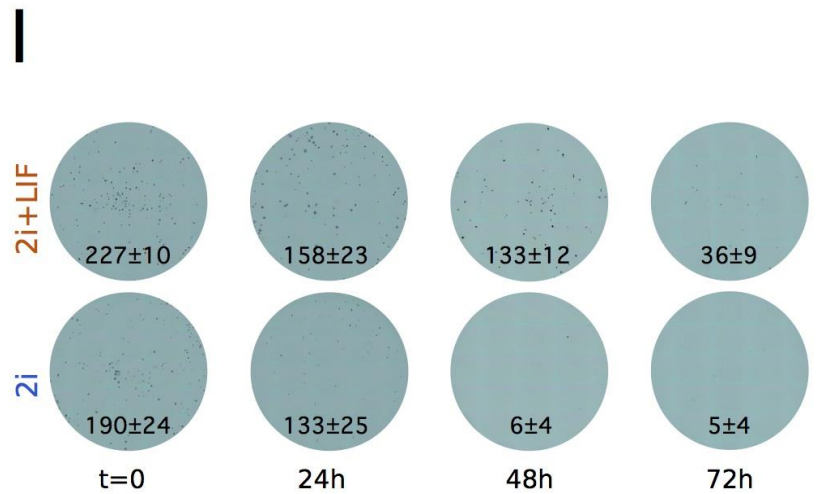
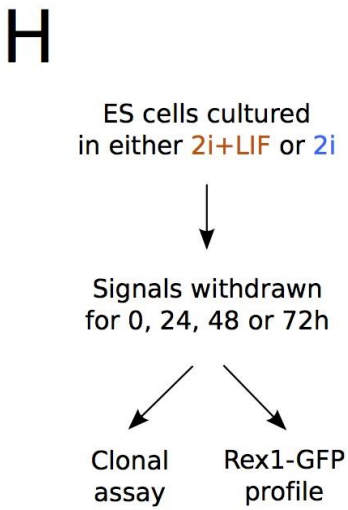
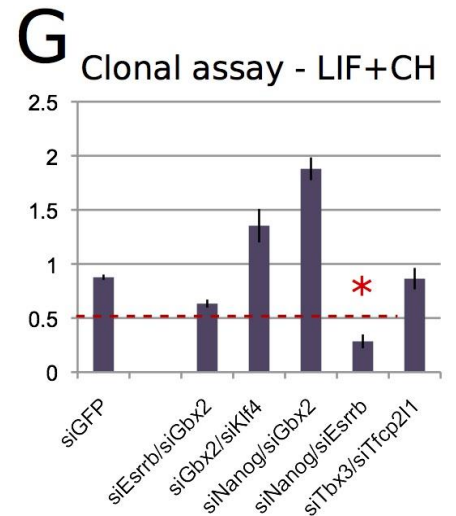
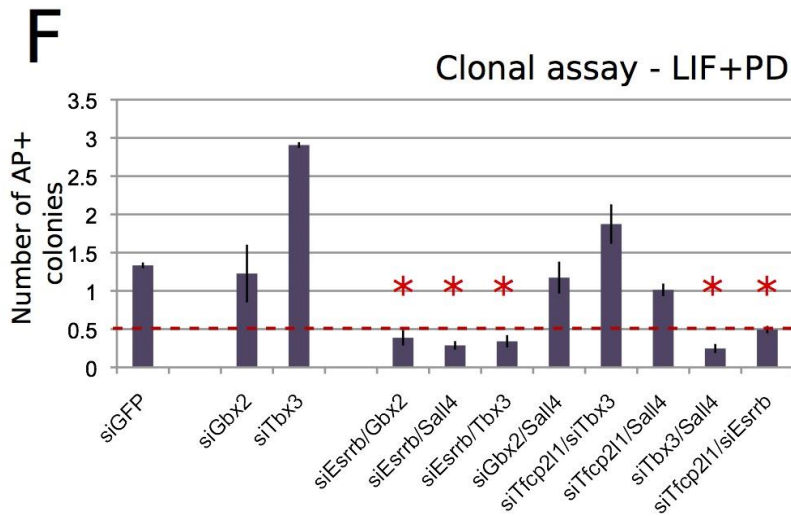
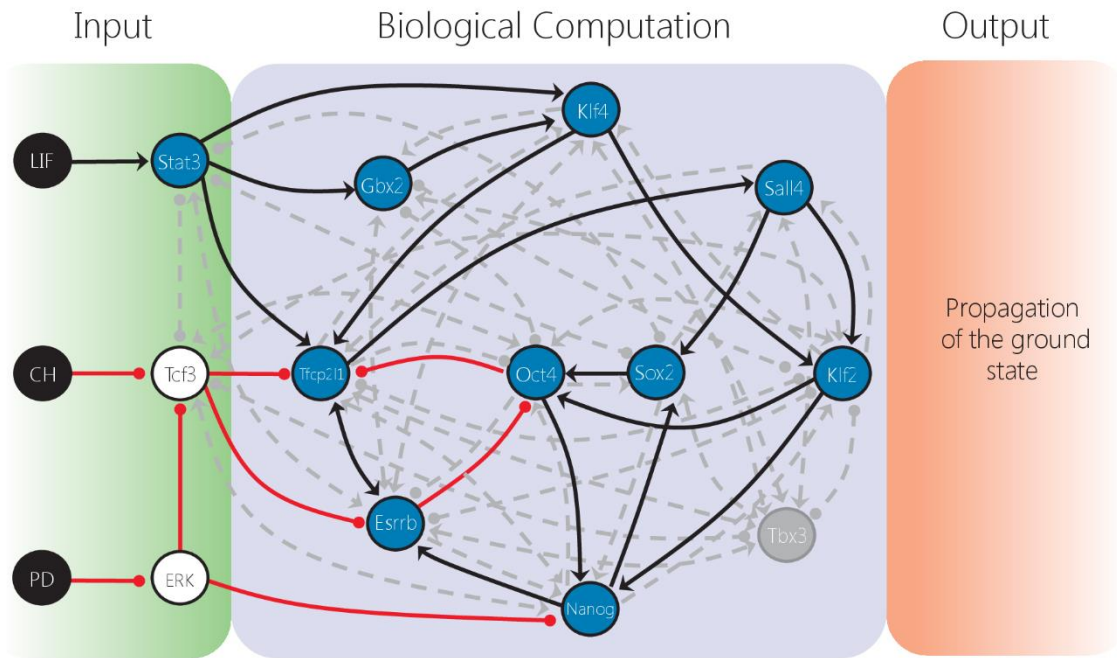


# Figure S6



**Supplementary Fig. S6:** (A-C) Clonal assays in 2i+LIF. The predictions involving loss of Nanog (panel B) or Tbx3 (panel C) have been tested both by double knockdown (right) and by single knockdown in cells lacking either Tbx3 or Nanog (left). Importantly, we obtained similar results from the two approaches. For each sample the number of AP+ colonies, relative to irrelevant siRNA transfected cells, is indicated. Each bar represents the mean and SEM of at least 4 independent experiments. (D) Additional predictions formed in 2i, which were not experimentally tested. (E) Clonal analysis of the indicated samples in 2i. Each bar represents the mean and SEM of at least 4 independent experiments. In all experiments only reductions >50% in ES cell colony formation (red dashed lines) are considered significant. (F) Clonal assay of ES cells in LIF+PD. Those indicated with a red asterisk correspond to incorrect model predictions. (G) Clonal assay of ES cells in LIF+CH. Only one wrong prediction was made in these conditions. Each bar represents the mean and SEM of at least 2 independent experiments. (H) Assessment of the stability of ES cells in 2i+LIF and 2i by plating in unsupplemented medium for 0, 24, 48 or 72 hours, and subsequently analysing the Rex1-GFP profile (Figure 3C), and replating for clonal assays in 2i + LIF (Figure S6I). (I) Clonal assay of cells maintained either in 2i+LIF or 2i and withdrawn for the indicated time, then replated in 2i+LIF. Representative wells are shown. Mean and SD are indicated (n=3). (J) Venn diagram showing the overlap of possible interactions as inferred from different sources. With no prior knowledge, there are 272 possible interactions between the 17 TFs. The set of possible, but still optional, interactions is reduced to 59 assuming the experimental constraints prescribed in Fig. 2B. Correspondingly, the set of consistent models derived represents a reduction by a factor of  $10^{64}$ .

# Figure S7



**Supplementary Fig. S7:** The constrained set of models that satisfy the original set of 23 specifications, in addition to the experimental data from knockdowns in 2i+LIF. The interactions that are highlighted correspond to the minimal model (Fig. 3D), while the interactions shown in grey define the remaining set of possible network models.

## **Materials and Methods**

### **S1A: Embryonic Stem Cell Culture**

ES cells were cultured without feeders on plastic coated with 0.1% gelatine (Sigma, cat. G1890) and replated every three days at a split ratio of 1 in 10 following dissociation with Accutase (PAA, cat. L11-007). Cells were cultured in serum-free media N2B27 (NDiff N2B27 base medium, Stem Cell Sciences Ltd, cat. SCS-SF- NB-02) supplemented, as indicated, with small-molecule inhibitors PD (1  $\mu$ M, PD0325901) and CH (3  $\mu$ M, CHIR99021) and LIF prepared in-house. Colony forming assays were carried out by plating 500 ES cells per well on plates coated with laminin (Sigma, cat. L2020). Plates were fixed and stained for alkaline phosphatase (Sigma, cat. 86R-1KT) according to the manufacturer's protocol. Plates were scanned using a CellCelector (Aviso) and scored manually.

### **S1B: Gene Expression Analysis by Quantitative RT-PCR with Reverse Transcription**

Cells were plated at a density of 15,000 cells/cm<sup>2</sup> and collected after 24h. Total RNA was isolated using the RNeasy kit (Qiagen) and 500 ng used for cDNA synthesis using SuperScript III (Invitrogen) and oligo-dT primers. Quantitative real-time PCR was carried out with SYBR green detection. Primers are detailed in Supplementary Table S1. Technical replicates were analysed for all reactions. Beta-Actin was used as an internal control and expression relative to the mean level of each gene has been calculated.



## **S1C: RNAi Experiments**

We performed siRNA transfection experiments to test the model predictions. ES cells were cultured in 2i+LIF and transfected with the indicated combinations of siRNAs (Fig. 3A, left panel). After 48h hours cells were counted and the same number of viable cells were plated at clonal density. The number of alkaline phosphatase positive (AP+) colonies formed after 5 days was counted. We used two different negative controls (an irrelevant siRNA and an anti-GFP siRNA). This assay provided a quantitative experimental measurement of the self-renewal capacity of ES cells (Fig. 3A, left panel, exp. validation column).

siRNAs were transfected at a final concentration of 40nM using Dharmafect 1 (Dharmacon, cat. T-2001-01), following the protocol for reverse transfection. For a 12 well plate (4cm<sup>2</sup>) we used 2 µl of transfection reagent, 2 µl of 20 µM siRNA solution and 30,000 ES cells in 1 ml of N2B27 medium. The medium was changed after overnight incubation. siRNAs were purchased from Qiagen and Ambion. For each gene we combined two pre-validated siRNAs to maximize knockdown efficiency (>65%, see Table S2).

## **S1D: Flow Cytometry**

After treatment with Accutase, live ES cells were resuspended in PBS with 3% FCS and ToPro-3 (invitrogen) was added at a concentration of 0.05nM to detect dead cells. Flow cytometry analyses were performed using a Dako Cytomation CyAn ADP high-performance cytometer with Summit software.

## **S1E: ChIP-seq and Microarray Data Analysis**

All raw and processed ChIP-seq data files, including lists of candidate target genes, used in Fig.S4C-D and S2A are available for download from [http://bioinformatics.cscr.cam.ac.uk/ES\\_Cell\\_ChIP-seq\\_compendium.html](http://bioinformatics.cscr.cam.ac.uk/ES_Cell_ChIP-seq_compendium.html).

Microarray data of ES cells after knockdown of single transcription factors, used in Fig. S3 and S4 are described in (11) and were obtained from <http://esbank.nia.nih.gov/download.html>.

## **S1F: Computational Approach**

The methodology for determining the architecture of the pluripotency program is shown in Fig. S1D. The challenge is to infer possible interactions between the pluripotency factors and to use experimental observations to determine which of these interactions are valid and necessary, and in what combinations.

First, we inferred optional interactions from gene expression data (Fig. 1B) and thereby constructed possible models of the network. Known experimental behaviour of ES cells was used to constrain this set (Fig. 2B), which was subsequently used to make predictions of ES cell behaviour in response to genetic perturbations. The predictions were experimentally tested (Fig. 3). This approach can be iterated to account for new experimental results, resulting in model refinement.

## **S1G: Abstract Boolean Networks**

To enable the automatic construction of computational models consistent with experimental observation, we developed an approach based on the application of formal synthesis procedures (12) to Boolean networks (13). We refer to the resulting models as Abstract Boolean Networks (ABNs). As in other Boolean formalisms, we represent TFs as network nodes, which can attain one of two levels at each time step (we use ‘low’ and ‘high’ to refer to these discrete gene expression levels). Directed edges in the network represent regulation interactions between TFs, which can be either positive (activation) or negative (inhibition). The network is considered ‘abstract’ because certain edges (referred to as ‘possible’) indicate only the option of an interaction between the nodes they connect, as opposed to the definite presence of such an interaction. Thus, an ABN with  $n$  possible interactions encodes  $2^n$  different concrete Boolean networks (BNs) and is used to represent the set of possible models of the pluripotency network.

The dynamics of ABN models are defined similarly to Boolean networks with synchronous updates. At each time step, the state of each node is determined through the application of a ‘regulation function’ - a Boolean function of all regulators to the node. We limit the choice of regulation functions to one of 15 predefined functions (Supplementary Table 3), constrained by assuming that (i) a gene can be active only when at least one of its activators is present (two special regulation functions were defined solely for Tcf3 and MEK/ERK, which do not have activators) and (ii) regulation is monotonic (e.g. a repressed gene does not become activated when additional repressors become available). For example, regulation function 4 states that a gene will be expressed only if all of its activators are expressed, but not all of its repressors. In contrast, regulation function 15 states that a gene will be expressed if at least one activator is expressed, and even if all of its repressors are expressed.

## **S1H: Reasoning about Abstract Boolean Networks**

Once a set of possible models is encoded as an ABN, we are interested in determining whether any concrete models from this set are consistent with experimentally observed behaviour (a synthesis problem) and generating predictions regarding the expected system behaviour (an analysis problem). We approached both types of questions by encoding ABNs and all additional constraints as Satisfiability Modulo Theories (SMT) problems. Similar strategies have been applied to tackle challenging problems arising in the verification and analysis of computer software and hardware, driving the development of efficient SMT solvers such as the Z3 theorem prover (21), which we use in this work.

The synthesis problem we consider corresponds to the identification of a concrete BN, where each possible interaction is set as present or not and the regulation functions of each node are instantiated. Furthermore, this BN must be capable of reproducing certain expected system behaviour (as in Fig. 2A). Given an ABN model and a set of additional constraints representing the required behaviour, the identification of concrete BN models is achieved automatically within our tool (see ‘Reasoning Engine for Interaction Networks’ below), while multiple consistent models can also be enumerated. Implicitly, the set of concrete BN models represented as an ABN is restricted through the additional constraints to a set of consistent models where only certain combinations of possible, i.e. optional, interactions are allowed, but the required behaviour is guaranteed.

Given an ABN constrained as described above, the analysis problem we consider for making predictions of the pluripotency network (see ‘Model Predictions’ below) amounts to deciding if

all concrete BN models from this set are capable of producing certain behaviour. This approach is conservative, since if a single concrete model from the set behaves differently, the analysis result is inconclusive. In general, this leads to fewer predictions than using a single concrete model but provides a more direct connection between experimental observations and the generated predictions, where all reasoning steps are based on formal logical rules and are performed automatically.

### **S1I: Reasoning Engine for Interaction Networks (RE:IN)**

This approach was implemented within a bespoke computational tool, RE:IN, a Reasoning Engine for Interaction Networks. This tool is targeted towards the analysis of biological systems such as gene regulation networks, represented as Boolean networks, allowing us to reason about the possible behaviour of such models for specific choices of interactions and dynamics. This functionality allows the identification of network interactions capable of reproducing certain experimentally observed behaviour, the interrogation of constrained model sets when multiple solutions are identified, and the generation of predictions of new behaviour under genetic perturbations. The tool is available for use from <http://research.microsoft.com/en-us/projects/rein/>, along with tutorials and example files required to run the analysis.

### **S1J: An ABN model of the Pluripotency Network**

The Pearson correlation coefficient was used as a metric to quantify the extent of correlation between any two TFs, and thereby to determine the possible interactions that comprise the set of models of the pluripotency network. For each gene pair, five Pearson correlation coefficients were determined: one for each set of experimental data (Fig. S3A).

An interaction was deemed possible if there existed at least one Pearson coefficient with absolute value above the defined threshold, and out of the remaining Pearson coefficients there was a majority of the same sign (i.e. positive or negative). The sign of the coefficient with maximum absolute value determines whether the interaction is an activation, or an inhibition. If this was not satisfied, then the interaction was deemed not to be present.

The Pearson coefficient does not indicate which gene out of the pair is the regulator. Therefore in the case of significant positive correlation between genes *A* and *B*, we must consider two possible cases: *A* activates *B*, and *B* activates *A*. Given that either interaction can be present, or not, there are four possible assignments to define a model of the network.

We found that the interactions suggested by a maximum Pearson correlation coefficient threshold of 0.792 were sufficient to satisfy the set of 23 experimental constraints (Fig. 2B). Furthermore, there were 11 interactions found to be present in all models that comprise this constrained meta-model. That is, we can conclude that without any one of these interactions, it would not be possible to satisfy the experimental constraints. These 11 interactions were also validated by available ChIP-Seq data (Section S2A).

### **S1K: Encoding Experimental Behaviour**

We defined a set of 23 experimental constraints, each derived from experimentally-observed behaviour (Fig. 2A). Fig. S3B illustrates the TF expression observed during one experiment, namely when CH is added to cells initially in LIF+PD. These cartoons illustrate both the set of

possible interactions (dashed lines) and the interactions that are assumed definite (solid lines), because they have previously been experimentally validated (see Fig. S1) (1–3, 5, 7, 8).

The full set of experimental constraints correspond to:

**1-12:** All possible conversions between the four different culture conditions (2i+LIF, 2i, LIF+CH, LIF+PD), where the gene expression patterns are those observed under steady state conditions.

**13-15:** Starting from conditions of 2i+LIF, 2i and LIF+PD and then removing all signals, we expect all TFs to have low expression at the final state.

**16-19:** Oct4, Sox2, Stat3 and Esrrb loss of function experiments under 2i conditions.

**20:** Esrrb knockdown in 2i+LIF.

**21:** Esrrb overexpression starting in 2i conditions, then removing CH.

**22:** Nanog knockdown in 2i+LIF.

**23:** Tfcp2l1 overexpression starting from 2i+LIF conditions, then removing LIF and CH (3, 5).

To encode these constraints, we first discretised the data so that the expression level of each gene was high (1) or low (0). For this discretisation, a threshold of 0.5 was used, above which the normalised gene expression was deemed to be high. Similarly, the presence or absence of the input signals LIF, CH and PD was encoded discretely in each case.

An initial state and a final state were defined for each experiment. Where a complete gene expression pattern is known, this was defined. However, in some cases, only a partial pattern is published. For these constraints, it was required only that those genes for which we know the expected expression should have a defined final state, and RE:IN did not constrain the remaining genes.

The trajectory length was fixed at 20 steps, which was sufficient to enable the individual solutions to converge to the expected final state. Furthermore, we required that the final state be visited in two successive time steps, which is sufficient to guarantee stabilisation for this class of systems when a complete gene expression pattern is defined, given trajectories are deterministic. Restricting the trajectory length could eliminate solutions that take longer to converge, which requires very specific, and potentially unrealistic, network topologies.

### **S1L: Model Predictions**

We made predictions of ES cell behaviour in response to genetic perturbations based on the behaviour of the entire constrained set of models.

Given that ES cells can tolerate the singular loss of several TFs, but neither of Oct4 or Sox2, we assumed that pluripotency is maintained only when Oct4 and Sox2 expression is high. To investigate whether single and double knockdowns would be tolerated we encoded candidate experimental constraints, and tested the set of models against these new constraints separately:

1. Both Oct4 and Sox2 are maintained under the knockdown.
2. Both Oct and Sox2 are not maintained under the knockdown.
3. Either Oct4 or Sox2 are not maintained under the knockdown.

First, we test (1). If we find solutions under this constraint, this does not reveal whether *all* of the models satisfy this constraint. Therefore we next test (2). If we find solutions to this constraint, then our results are inconclusive and we cannot form a prediction of the response of the network, because a subset of the solutions lead to maintenance of pluripotency, while a different subset



lead to loss of pluripotency. If we do not find solutions to (2), we then test (3), to ensure that it is not the case that either Oct4 or Sox2 are downregulated by any solutions. If (2) and (3) agree, and no solutions are found, then we predict that pluripotency is sustained. Likewise, if there are no solutions that satisfy (1), but solutions are found for (2) and (3), then we predict that pluripotency is always lost.

### **S1M: Refining the Meta-Model**

Adding additional interactions to the meta-model (e.g. by lowering the Pearson correlation threshold) increases the number of unique instantiations of interactions, i.e. the number of possible models. Since we only make predictions when all of the models agree, the predictive power of the meta-model could decrease as interactions are added, as this subsequently increases the number of unique models that can produce different behaviours.

This approach motivates our desire for the minimal set of interactions that can satisfy all 23 experimental constraints, and hence why we use a Pearson correlation threshold of 0.792 to define the meta-model. For example if we pick a low Pearson correlation threshold, such as 0.6, we do not generate any predictions of the network response to genetic knockdowns.

A further refinement of the meta-model is required if the set of models cannot satisfy the set of experimental constraints. This was necessary to account for the model prediction of Tbx3/Klf2 double knockdown, which was incorrectly predicted to result in loss of self-renewal. The general approach is to incrementally lower the Pearson correlation threshold to identify which interactions are required to satisfy this additional, new constraint. However, in keeping with our

aim to keep the simplest, and therefore predictive, meta-model, we sought not to include additional interactions that were unnecessary to satisfy this constraint.

A maximum Pearson correlation coefficient threshold of 0.647 generated a set of possible interactions that defined a meta-model that could satisfy the new constraint. However, out of the set of interactions that were introduced by lowering the threshold, only one interaction was necessary: an optional, positive interaction between Oct4 and Sox2. Thus, the refined set of models was still defined by a threshold of 0.792, but with this additional possible interaction. Note that this interaction is consistent with ChIP-Seq data.

### **S1N: Minimal Model**

RE:IN allows us to limit the number of interactions that constitute model solutions we seek. An alternative approach would be to limit the number of components that constitute model solutions we seek. We firstly identified that there were no models with fewer than 17 interactions, and RE:IN identified 2 models of this size. However, Tbx3 does not act as a regulator in either of these model solutions. Removing those interactions involving Tbx3 from each model produced an identical set of interactions, which is that shown in Fig. 3D.

While Tbx3 is not required to act as a regulator in all of the models that constitute the meta-model, and in particular, can be eliminated from the minimal model, this is not the case for Gbx2. Rather, Gbx2 is required to satisfy all of the experimental constraints and must be present in every model solution. In the minimal model, Gbx2 acts in a feedforward loop from Stat3 to Klf4, and so its presence is required to mediate the proper regulation of Klf4. This is an effect

that propagates through the network before Klf4 can no longer act as a regulator, in order to satisfy the complete set of experimental observations.

## Supplementary Text

### S2A: Initial Validation of Possible Network Interactions

As an alternative to examining gene expression of ES cells cultured in equivalent conditions that each preserve pluripotency, the topology of a network can be interrogated by genetic perturbations. Those genes that are differentially expressed upon knockdown and/or overexpression are deemed to be regulated by the gene that is perturbed. To determine whether our set of inferred interactions are supported by such experiments, we accessed open-source microarray data of gene expression profiles of ES cell lines following genetic perturbations (11). For example, our comparison of culture conditions suggested 6 possible, positive interactions involving Nanog (Fig. S4A). Upon Nanog loss of function 3 out of the 6 genes were reported to be downregulated (Fig. S4B).

We repeated the same procedure for each proposed interaction, and found that 44% of the possible interactions we proposed were validated by the perturbation studies (Fig. S2A). This degree of accuracy is high, given that gene expression correlation alone does not expose directionality and therefore maximum validation is 50%. Inferred interactions are assumed to be functional, but not necessarily direct. Nevertheless, when we interrogated available ChIP-Seq data (Fig. S4C) we found that 73% of interactions have been detected in terms of TFs binding to target gene loci, and therefore may be direct (Fig. S2A). Notably, this includes the 11 interactions that we inferred to be required for the pluripotency network (Fig. 2B). Therefore the set of possible interactions that we found to be sufficient to generate models that can explain known ES cell behaviour (Fig. 2B) are supported by independent data.

As a control, we generated the complete list of interactions inferred only from the open-source genetic perturbation data, which totals 81 (Fig. S4D). Importantly, when we used these

interactions to build a new set of models as before, the tool determined that no models from this set could satisfy the 23 experimental constraints. This is despite there being a greater number of models compared to those inferred from our gene expression correlation data. We suggest that significant interactions can be more reliably captured by comparing homogeneous populations of ES cells under different culture conditions (as in Fig. 1), than from genetic perturbation studies on mixed populations of differentiated and self-renewing cells.

We compared our computational approach to Bayesian network inference, a common formalism for investigating and reconstructing regulatory networks (9, 10, 14–18). We applied a freely-available Bayesian network inference method, previously used to study somatic cell reprogramming (10). This approach yielded fewer interactions and generated only one model. Crucially that model is not consistent with known experimental behaviour (Fig. S2B). For instance, Oct4 and Sox2 are not connected to external signals.

### **S2B: Non-intuitive predictions**

Our approach generated non-intuitive predictions. For example, the combined knockdown of Sall4 and Klf2 was predicted to compromise self-renewal in 2i+LIF. To test this experimentally, we first knocked down Sall4 and Klf2 individually and found that Sall4 downregulation resulted in a mild reduction in the number of AP+ colonies, compared to the control siRNAs, whereas Klf2 downregulation had no effect (Fig. 3B). However, double knockdown of Klf2 and Sall4 significantly reduced the self-renewal capacity of ES cells, matching the prediction from the set of models. Of note, the synthetic effect of the Klf2/Sall4 double knockdown could not be inferred from the single knockdown results, highlighting the power of our approach.

### **S2C: Extended Discussion**

Naïve pluripotency is a fleeting state in the developing blastocyst that can be sustained *in vitro* in mouse ES cells under the influence of three different signals: LIF, CH and PD. These signals are not equivalent and maintain pluripotency via different signalling pathways, yet only two of the three are required. Furthermore, ES cells can efficiently transit between the different signal combinations. To-date, the field has amassed considerable information on the transcriptional regulators that are associated with the control of this state, and the signalling pathways that are modulated by these culture conditions. But we have yet to provide a predictive explanation of the regulation of the self-renewing state.

Here we implemented a powerful, computational approach by integrating formal synthesis procedures (12) within a modelling framework based on Boolean networks (19), and utilised an unique experimental system that allowed us to compare homogeneous pluripotent cell populations to investigate the possible interactions that regulate self-renewal. By integrating computationally gene expression data characterising the self-renewing state with known perturbation phenotypes, we derived possible combinations of interactions that suffice to explain observed ES cell behaviour. These suggested interactions are substantiated both by ChIP-Seq and genetic perturbation data. By virtue of the formal verification procedures we implemented, each possible model is proven to capture all of the observed experimental behaviour. Thus we derived a set of consistent, unique, candidate models of the pluripotency program, which together constitute a ‘meta-model’ of naïve pluripotency.

Between the set of 17 TF initially considered, with no prior knowledge of gene interaction there are  $10^{46}$  possible models of the network. This is an intractable number of models to interrogate manually, and moreover, would not yield any predictions of ES cell behaviour. We used the meta-model in a robust approach to identify and constrain only those interactions and components that are necessary to sustain naïve pluripotency. As such, we refine, not a single

model, but the set of possible models. Through this analysis, the number of possible models was greatly reduced, by a factor of  $10^{25}$ . Moreover, the meta-model was sufficiently constrained to form non-intuitive, but accurate predictions of the system behaviour under the action of compound perturbations.

The Pearson correlation coefficient is applied within this methodology to identify possible interactions between gene pairs, and the same interactions were validated by independent experimental techniques. It is possible that more complex behaviour such as pulse-activation or a time-delayed response exists between genes, and this would not be captured by the Pearson coefficient. However, this has not emerged as an issue for the constrained set of models, which was able to accurately explain ES cell behaviour and generate new predictions.

Recent reports showed that ES cell core factors, such as Nanog, undergo self-regulation (Navarro et al., 2012). This prompted us to examine the consequence of adding self-regulation loops by including optional positive and negative self-regulation to each gene. We then re-ran our analysis to examine whether a difference arose in the set of predictions that were obtained under 2i/LIF conditions. We found that 10 double knockdown predictions were generated in total, compared to the 11 we found without these loops. 8 of these recapitulated predictions that we had already generated (including the incorrect prediction that Tbx3/Klf2 double knockdown leads to loss of self-renewal), and the remaining 2 were predictions that we did not generate before. Therefore, allowance for auto-regulation has not improved predictive power; even if the two new predictions are correct, the addition of self-regulatory loops would generate 9 out of 10 correct predictions, compared to 11 out of 12 (Fig. 3A, left panel).

Our results reveal that ES cell decision-making is not necessarily dependent on a vast genetic network, as widely considered, but instead can be explained by a program that, in its simplest version, consists of just 16 interactions, 12 components and 3 inputs. This example model from the meta-model identifies the minimal essential network that can maintain naïve pluripotency under four different culture conditions. Environmental signals are processed via the interactions between pluripotency factors to stabilise the gene expression pattern that characterises a self-renewing, pluripotent cell (Fig. 3D). As such, the program itself is unchanging under the action of different inputs, but determines the appropriate stable state as a consequence of these inputs.



Table S1 – Primers used for Real-time quantitative RT-PCR

Gene Name	Forward	Reverse
Beta-actin	ctaaggccaaccgtgaaaag	accagaggcatacaggga
Klf2	ctaaaggcgcattctgcgta	tagtggcgggtaagctcgt
Klf4	cggaaggaggagaagacact	gagttcctcacgccaacg
Klf5	ccggagacgatctgaaacac	cagatacttctccatttcacatctg
Nanog	ttcttgcttacaagggtctgc	agaggaaggggcgaggaga
Nr0b1 (Dax1)	cgtgctctttaaccagacc	ccggatgtgctcagtaagg
Pou5f1	gttggagaagggtggaaccaa	ctccttctgcagggtttc
Rex1 (Zfp42)	tcttctctcaatagagtgagtgtgc	gctttcttctgtgtgcagga
Sox2	tccaaaaactaatcacaacaatcg	gaagtgcattgggatgaaaa
Tfcp2l1	ggggactactcggagcatct	ttccgatcagctcccttg
Esrrb	ggcgttctcaagagaacca	cccactttgaggcatttcat
Gbx2	ggcacctcctagatgtggac	aaaacactgcagctgagatcc
Tbx3	ttgcaaagggttttcgagac	tgcagtgtgagctgctttct
Tcf3 (Tcf7l1)	ctgagcagcccgtacctct	aggggccatttcattctgtag
Sall4	gaagccccagcacatcaac	ctgaggcttcacgcagtt
Stat3	gtcctttccaccaagtga	tatcttggccctttggaatg
Mi2b (CHD4)	gccaatgcagctctacacaa	tgtaacctcacagcgactgg
Mb3	agaagaaccctggtgtgtgg	tgtaccagctcctctgctt

Table S2 – siRNA

Name	Supplier	Cat. Number
Negative	Qiagen	1027280
siGFP	custom (target sequence GCAAGCTGACCTGAAGTTCA)	
Klf2_A	Qiagen	SI01083530
Klf2_B	Qiagen	SI01083544
Klf4_A	Qiagen	SI01083544
Klf4_B	Qiagen	SI01083593
Esrrb_A	Qiagen	SI02672110
Esrrb_B	Qiagen	SI02739569
Nanog_A	Qiagen	SI04460869
Nanog_B	Qiagen	SI01323357
Tfcp2l1_A	Qiagen	SI01444296
Tfcp2l1_B	Qiagen	SI04401558
Tbx3_A	Ambion	AM16708/223884
Tbx3_B	Ambion	AM16708/223885
Sall4_A	Qiagen	SI01409863
Sall4_B	Qiagen	SI01409877

Gbx2_A	Qiagen	SI01010170
Gbx2_B	Qiagen	SI01010177

Table S3 – Antibodies used in Figure 1A and S2A-C  
 Immunostaining was performed as previously described (Martello et al, 2012 *Cell Stem Cell*)

Target protein	Catalogue Number	Concentration
Nanog (rat)	MLC-51 (Ebioscience)	1:200
Oct4 (mouse)	5279 (Santa Cruz)	1:200
Esrrb	pp-H6705-00 (Perseus)	1:400

LOGIC NUMBER	Target gene not repressible and at least one activator is present.	Target gene not repressible but all activators are present.	No repressors present. At least one activator present.	No repressors present. All activators present.	At least one activator present and at least one, but not all, repressors present.	At least one activator present and all repressors present.	All activators present, at least one repressor present.	All activators and repressors present.	Not inducible. No repressors present.	Not inducible. At least one, but not all, repressors present.
0										
1										
2										
3										
4										
5										
6										
7										
8										
9										
10										
11										
12										
13										
14										
15										
16										
17										

Table S3 - Regulation functions. Each gene can influence those genes it interacts with by any one of fifteen possible regulations logics. There is a unique choice of logic for each gene, per model. It is assumed that no gene can be activated without at least one activator present. The regulations logics define the conditions under which a gene can be activated, according to the presence / absence of those genes which regulate its activity. The logics span the range of regulation functions under this assumption. The red boxes indicate where the conditions under which a given logic will allow a gene to become activated. Two additional regulation functions are defined only for Tcf3 and MEK/ERK, which do not require activators.

**Additional References**

1. J. Hall *et al.*, Oct4 and LIF/Stat3 additively induce Krüppel factors to sustain embryonic stem cell self-renewal., *Cell Stem Cell* **5**, 597–609 (2009).

2. C.-I. Tai, Q.-L. Ying, Gbx2, a LIF/Stat3 target, promotes reprogramming to and retention of the pluripotent ground state., *J. Cell Sci.* **126**, 1093–8 (2013).
3. G. Martello, P. Bertone, A. Smith, Identification of the missing pluripotency mediator downstream of leukaemia inhibitory factor., *EMBO J.* , 1–14 (2013).
4. J. Wray *et al.*, Inhibition of glycogen synthase kinase-3 alleviates Tcf3 repression of the pluripotency network and increases embryonic stem cell resistance to differentiation., *Nat. Cell Biol.* **13**, 838–45 (2011).
5. G. Martello *et al.*, Esrrb is a pivotal target of the Gsk3/Tcf3 axis regulating embryonic stem cell self-renewal., *Cell Stem Cell* **11**, 491–504 (2012).
6. Q.-L. Ying *et al.*, The ground state of embryonic stem cell self-renewal., *Nature* **453**, 519–23 (2008).
7. F. Lanner *et al.*, Heparan sulfation-dependent fibroblast growth factor signaling maintains embryonic stem cells primed for differentiation in a heterogeneous state., *Stem Cells* **28**, 191–200 (2010).
8. J. Silva *et al.*, Nanog is the gateway to the pluripotent ground state., *Cell* **138**, 722–37 (2009).
9. B. Wilczyński, N. Dojer, BNFinder: exact and efficient method for learning Bayesian networks., *Bioinformatics* **25**, 286–7 (2009).
10. Y. Buganim *et al.*, Single-cell expression analyses during cellular reprogramming reveal an early stochastic and a late hierarchic phase., *Cell* **150**, 1209–22 (2012).
11. A. Nishiyama *et al.*, Systematic repression of transcription factors reveals limited patterns of gene expression changes in ES cells., *Sci. Rep.* **3**, 1390 (2013).
12. A. Church, in *Proceedings of the international congress of mathematicians*, (1962), pp. 23 – 35.
13. S. a Kauffman, Metabolic stability and epigenesis in randomly constructed genetic nets., *J. Theor. Biol.* **22**, 437–67 (1969).
14. K. Missal, M. a Cross, D. Drasdo, Gene network inference from incomplete expression data: transcriptional control of hematopoietic commitment., *Bioinformatics* **22**, 731–8 (2006).
15. N. Friedman, M. Linial, I. Nachman, D. Pe’er, Using Bayesian networks to analyze expression data., *J. Comput. Biol.* **7**, 601–20 (2000).
16. Y. Liu *et al.*, A novel Bayesian network inference algorithm for integrative analysis of heterogeneous deep sequencing data., *Cell Res.* **23**, 440–3 (2013).
17. A. A. Margolin *et al.*, ARACNE: an algorithm for the reconstruction of gene regulatory networks in a mammalian cellular context., *BMC Bioinformatics* **7 Suppl 1**, S7 (2006).

18. J. Yu, V. A. Smith, P. P. Wang, A. J. Hartemink, E. D. Jarvis, in *International Conference on Systems Biology*, (2002).
19. S. a Kauffman, Metabolic stability and epigenesis in randomly constructed genetic nets., *J. Theor. Biol.* **22**, 437–67 (1969).